

Magneto-optical effects in nickel and Permalloy associated with frustrated total internal reflection

G. S. Krinchik, E. E. Chepurova, and T. I. Kraeva

M. V. Lomonosov State University, Moscow

(Submitted 30 January 1985)

Zh. Eksp. Teor. Fiz. **89**, 277–285 (July 1985)

Magneto-optic effects accompanying frustrated total internal reflection are investigated in transversely (equatorial Kerr effect δ^E) and longitudinally (meridional intensity effect δ^{MI}) magnetized nickel and Permalloy samples for light incident at $15 < \varphi < 85^\circ$ and photon energies $1.5 < \hbar\omega < 3.2$ eV. The magneto-optical spectra are compared for transversely and longitudinally magnetized samples, and the influence of the dielectric constant of the material adjacent to the magnetic film is analyzed. The minima observed in the reflection curves are attributed to the excitation of surface plasma waves (SPW), while the extrema in the magnetoreflexion curves are ascribed to surface magnetoplasma waves (SMPW). The dispersion curve $k(\omega)$ for transversely magnetized samples is found to split into high- and low-energy branches (here k is the wave vector of the SPW). For longitudinally magnetized samples, only one branch $k(\omega)$ is observed for surface magnetoplasma waves, in agreement with theoretical predictions. Dispersion equations for surface magnetoplasma waves are derived for $1.5 < \hbar\omega < 3.2$ eV. The wave vectors of the SMPWs are found to increase with ε , the dielectric constant of the material at whose boundary the SPW and SMPW waves are generated; moreover, the splitting Δk induced by a transverse magnetic field $\pm H$ becomes smaller as ε increases.

INTRODUCTION

Surface polaritons are coupled polarized electromagnetic (EM) modes that propagate as waves along the interface between two media and decay exponentially with distance from the surface.¹⁻⁴ In particular, EM radiation incident on a metal surface may excite a surface plasma wave (SPW), because the discontinuity of the electric field component normal to the interface causes the surface charge to oscillate. The dispersion equation

$$k = (\omega/c) [\varepsilon_1 \varepsilon_2 / (\varepsilon_1 + \varepsilon_2)]^{1/2}, \quad (1)$$

for the SPWs can be derived by solving the Maxwell equations with appropriate boundary conditions. Here k is the wave vector of the SPW, ω is the frequency of the incident light, c is the speed of light in vacuum, and ε_1 and ε_2 are the dielectric constants of the two media. In order for a surface wave to exist, we must have $\text{Re}(\varepsilon) < 0$ in one of the media (the surface-active medium), i.e., the wave vector of the SPW is greater than k for the incident light. Surface plasma waves therefore cannot be excited by light reflected by a surface-active material forming an interface with an inactive medium.

The method of frustrated total internal reflection (FTIR) proposed by Otto⁵ is widely employed to excite SPWs in metals and semiconductors. In the Otto configuration the metal (or semiconductor) lies a distance $d \sim \lambda$ from the base of a prism at which the light undergoes total internal reflection (TIR). At TIR a nonuniform exponentially decaying wave forms in the optically less dense medium (air) and excites a SPW at the air-metal (air-semiconductor) interface. In Kretschmann's modification,⁶ a thin surface-active film is deposited directly on the base of the prism, and a SPW is again excited at the air-metal interface. In either case, the experimental configuration permits the wave vectors (phase velocities) of the SPW to be synchronized with

the optical wave, which propagates parallel to the base of the prism. As a result, some of the energy of the incident light is used to excite an SPW, and the total internal reflection is attenuated. The wave vector of the SPW is then given by

$$k = (\omega/c) N \sin \varphi, \quad (2)$$

where N is the refractive index of the prism and φ is the incident angle at which the reflection coefficient for p -polarized light (TH mode) is a minimum. We note that the SPW spectrum is more complicated for a triple-layer structure (e.g., prism-metal-air) and is described by the equation⁷

$$\left(\frac{\varepsilon_1}{\alpha_1} + \frac{\varepsilon_2}{\alpha_2} \right) \left(\frac{\varepsilon_3}{\alpha_3} + \frac{\varepsilon_2}{\alpha_2} \right) - \left(\frac{\varepsilon_1}{\alpha_1} - \frac{\varepsilon_2}{\alpha_2} \right) \left(\frac{\varepsilon_3}{\alpha_3} - \frac{\varepsilon_2}{\alpha_2} \right) e^{-2\alpha_2 t} = 0, \quad (3)$$

where

$$\alpha_1^2 = k^2 - k_0^2 \varepsilon_1, \quad \alpha_2^2 = k^2 - k_0^2 \varepsilon_2, \quad \alpha_3^2 = k^2 - k_0^2 \varepsilon_3, \quad k_0 = \omega/c.$$

Here k is the wave vector of the surface plasma wave; ε_1 , ε_2 , ε_3 are the dielectric constants of the prism, metal, and air, respectively; t is the thickness of the metal film.

The surface plasma waves become surface magnetoplasma waves (SMPW) when an external H field is applied. Moreover, their dispersion equations depend on the angle between H and the wave vector of the SPW and the incident plane of the light. In particular, if the Drude model is used to describe the dielectric tensor, one can show^{8,9} that if $\mathbf{H} \parallel \mathbf{k}$ (external magnetic field normal to the plane of incidence and direction of propagation of the SPW), the dispersion curve splits into a high- and a low-energy branch, depending on the sign of H . Surface magnetoplasma waves in semiconductors as well-understood theoretically^{8,9} and have been observed experimentally.^{10,11} However, almost no work has been done for ferromagnetic metals, in which an internal molecular field excites the SMPW. We can cite only Refs. 12 and 13, in which SMPW dispersion equations are derived

and the observation of the high-energy SMPW branch is reported for nickel. We note that the excitation of SPWs in Refs. 12 and 13 corresponded to a minimum in the reflection curve at FTIR, while SMPW excitation was accompanied by an abrupt increase in the magnetoreflexion (equatorial Kerr effect). Magneto-optical techniques for analyzing magnetic materials are known to be particularly effective for studying the interaction of light with magnetically ordered materials and for probing the structure and properties of surfaces. It will therefore be of great interest to analyze magneto-optical effects at FTIR in ferromagnetic metal films, and this is the purpose for the present paper. We compare the magneto-optical spectra for transversely and longitudinally magnetized samples and study how they are altered by the properties of the dielectric adjacent to the magnetic film.

SAMPLES AND MEASUREMENT TECHNIQUE

We used a magneto-optical setup, based on a DMR-4 monochromator and described in detail in Ref. 14, to measure the intensity of the reflected light as a function of frequency and angle for $H \parallel k$ (equatorial Kerr effect, EKE) and $H \perp k$ (meridian intensity effect, MIE).¹⁴ Light of energy $1.5 < \hbar\omega < 3.2$ eV was incident at angles $\varphi = 15\text{--}85^\circ$ on the thin ferromagnetic film samples. The measurements were made in Kretschmann's FTIR configuration.⁶

The nickel and Permalloy film samples were vacuum-sputtered on the flat surface of a glass half-cylinder (diameter 7 mm, refractive index $N = 1.7$) and were mounted so that the cylinder axis was parallel to the monochromator slit. A system of lenses focused the light to a point a distance d ahead of the curved cylinder surface, where d was chosen so that the light beam was parallel inside the cylinder.¹⁵ The films were mounted on a special rotating platform so that φ could be specified to within 0.5° , and they ranged in thickness from 160 to 2000 Å. Liquid dielectrics—water ($n = 1.33$), oil of cedar ($n = 1.515$), and mercury—were added to a cell adjacent to the metal-air interface.

The familiar formula

$$\delta = \Delta R / R \quad (4)$$

determines the magnitude of the EKE and MIE effects; here ΔR is the change in the intensity of the reflected light due to the magnetization of the film, and R is the intensity of the reflected light intensity for $H = 0$.

The reflection coefficient for a thin film is given by

$$R = (r_1 + r_2 e^{-i2\Delta}) / (1 + r_1 r_2 e^{-i2\Delta}), \quad (5)$$

where r_1 and r_2 are the reflection coefficients at the glass-film and film-dielectric interfaces, respectively; the phase factor $\Delta = 2\pi n^* t \cos(\varphi) / \lambda_0$ is proportional to the film thickness; $n^* = n + ik$ is the complex refractive index of the film; φ is the angle of refraction, and λ_0 is the light wavelength in vacuum. When an external magnetic field is applied, r_1 and r_2 change and expression (5) takes the form

$$R^\pm = (r_1^\pm + r_2^\pm e^{-i2\Delta}) / (1 + r_1^\pm r_2^\pm e^{-i2\Delta}), \quad (6)$$

where the \pm signs correspond to the two opposite directions $\pm H$ of the field.

In this case the change in the intensity of the reflected light due to the magnetization of the film is given by

$$\delta = (|R^+|^2 - |R^-|^2) / 2|R|^2. \quad (7)$$

We measured the EKE for the p -component of the incident light; the meridian intensity effect was nonzero for incident polarizations intermediate between the p - and the s -polarizations.¹⁴

EXPERIMENTAL RESULTS AND DISCUSSION

We measured δ in Ref. 16 for longitudinally and transversely magnetized nickel films of thickness $t = 2000$ and 160 Å; we also measured the angular dependence $R_p/R_s(\varphi)$, where R_p and R_s are the reflection coefficients for p - and s -polarized light. Since R_s depends monotonically on φ , the $R_p/R_s(\varphi)$ curves essentially reflect the behavior of $R_p(\varphi)$. For a nickel film with $t = 2000$ Å, $R_p/R_s(\varphi)$ had the typical form for reflection by a (glass-air) interface with a nonzero absorption coefficient. For $t = 160$ Å we recorded a sharp increase in R_p/R_s at $\varphi = 36^\circ$, which coincided with total internal reflection of the light at the nickel-air interface ($\varphi_{cr} = \arcsin(1/N)$), and there was a deep minimum for $\varphi = 55\text{--}65^\circ$. According to Ref. 4 and the data in Refs. 12 and 13, this minimum is caused by the frustration of total internal reflection that accompanies the excitation of surface plasma waves at the Ni-air interface. A sharp (3–5)-fold increase in δ for the equatorial Kerr effect was observed on either side of the peak in R_p/R_s , and the enhancement was attributed to excitation of surface magnetoplasma waves. Figure 1b shows the dispersion $k(\omega)$ calculated by Eq. (2) for the two SMPW branches for a nickel film, $t = 160$ Å.

Figure 1a shows the angular dependences $\delta^E(\varphi)$ for a nickel film with $t = 160$ Å recorded with a water-filled cell ($n_3 = \varepsilon_3^{1/2} = 1.33$). Curve 1 in Fig. 2 shows a typical result for $R_p/R_s(\varphi)$ for $\hbar\omega = 3.2$ eV. We see that in this case R_p/R_s rises abruptly at $\varphi = 51^\circ$, which corresponds to TIR for the p -component of the light incident at the Ni-water interface, while the deep minimum (caused by SPW excitation at the Ni-water interface) lies at $\varphi = 60\text{--}70^\circ$. We note that the formula $\varphi_{cr} = \arcsin(\varepsilon_3/\varepsilon_1)^{1/2}$ gives the TIR angle for light incident on the film-dielectric interface for the prism-film-dielectric configuration used in the experiment (here ε_1 and ε_3 are the dielectric constants of the prism and dielectric, respectively). The experimental value $\varphi \approx 51^\circ$ agrees with the calculated result $\varphi = \arcsin(1.33/1.7)$. The minimum value of R_p/R_s in this case is roughly 50% of the minimum for curve 2, which was recorded with an air-filled cell. In general, the depth of the minimum in $R_p/R_s(\varphi)$ is very sensitive to the film thickness. The above result thus shows that the depth of the minimum in $R_p/R_s(\varphi)$ can be adjusted by selecting a suitable dielectric while leaving the thickness t unchanged (this is much easier than changing t).

Figure 1b shows the dispersion $k(\omega)$ for the two branches of the SMPW. Here $k(\omega)$ was also calculated by Eq. (2) with φ chosen to maximize δ_E for a fixed energy $\hbar\omega$. The solid curves show $k(\omega)$ for an air-filled cell. We see that the maximum energy splitting $\Delta(\hbar\omega)$, equal to 0.6 eV for an air-filled cell, drops to 0.15 eV for a water-filled cell.

We also measured δ^{MI} for the meridional intensity effect. In this case the cell was alternately filled with water and

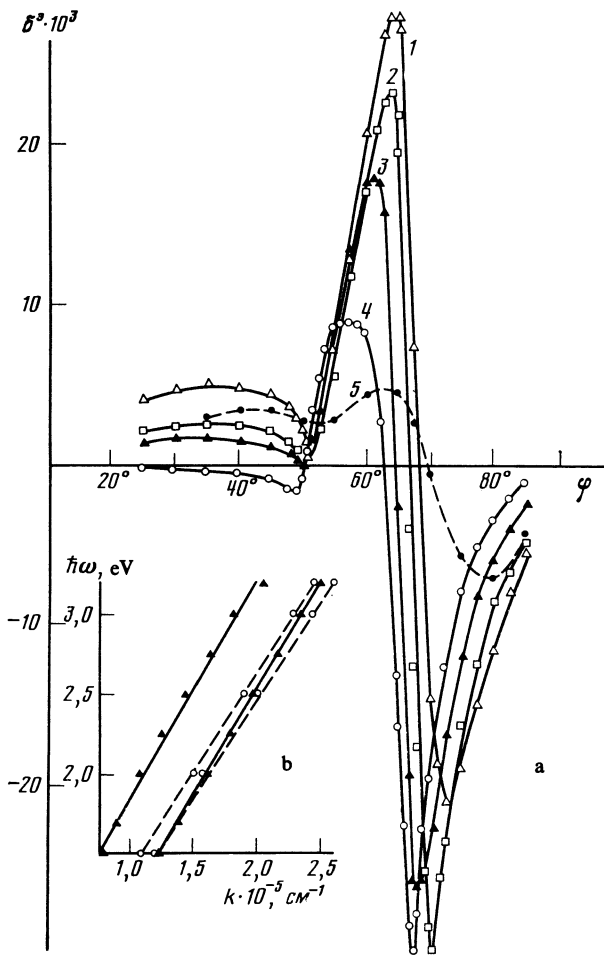


FIG. 1. a: Angular dependence $\delta^E(\varphi)$ in nickel for $t = 160 \text{ \AA}$; curves 1–4 correspond to $\hbar\omega = 3.2, 2.5, 2.0,$ and 1.5 eV , respectively, for a water-filled cell ($\epsilon_3 = 1.77$); curve 5 is for $\hbar\omega = 3.2 \text{ eV}$, mercury-filled cell. b: Dispersion curves $k(\omega)$ for surface magnetoplasma waves in nickel for $\epsilon_3 = 1$ (\blacktriangle) and $\epsilon_3 = 1.77$ (\circ).

oil. As in the case of air-filled cells,¹⁶ we found that for longitudinally magnetized films δ^{MI} had only a single maximum, which occurred for φ close to the minimum R_p/R_s . This increase in δ^{MI} for a thin film was attributed to excitation of a single SMPW branch, in qualitative agreement with Refs. 8 and 9, where it was concluded theoretically that the spectrum $k(\omega)$ should not split into two branches for longitudinally magnetized magnetically active materials.

We note that the curve $\delta^E(\varphi)$ for a mercury-filled cell on a nickel film with $t = 160 \text{ \AA}$ (Fig. 1) was nearly identical to $\delta^E(\varphi)$ for an Ni film with $t = 2000 \text{ \AA}$. This curious result can be explained by noting that mercury is optically denser than the nickel for energies $\hbar\omega = 1.5\text{--}3.2 \text{ eV}$, so that total internal reflection does not occur at the nickel-mercury interface. Since no SMPWs or SPWs are excited, there are no peaks or dips in $\delta^E(\varphi)$ and $R_p/R_s(\varphi)$.

The expression

$$\delta_t^E = \text{Re} \left[(\delta^E - i\delta^I) \frac{1 - (1+r_2)e^{-i2\Delta} - r_2^2 e^{-i4\Delta}}{1 - 2qr_2 e^{-i2\Delta} + r_2^2 e^{-i4\Delta}} \right] \quad (8)$$

for the magnitude of the equatorial Kerr effect in a film of finite thickness can be derived from Eqs. (6), (7) if we recall

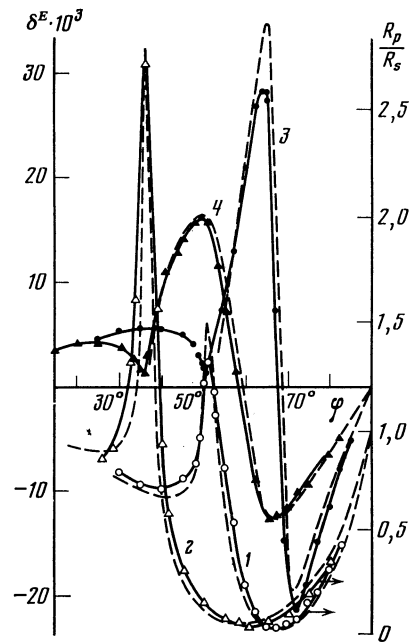


FIG. 2. Angular dependences $R_p/R_s(\varphi)$ (1,2) and $\delta^E(\varphi)$ (3,4) for nickel. Curves 2, 4, are for $\epsilon_3 = 1$, curves 1, 3 correspond to $\epsilon_3 = 1.77$. The solid and dashed curves give experimental and calculated values, respectively ($\hbar\omega = 3.2 \text{ eV}$, $t = 200 \text{ \AA}$, $\epsilon_1 = 2.89$, $\epsilon_3 = 1.69$, $\epsilon_2 = -2.35 + i0.105$; $\epsilon_2' = 0.0325 + i0.101$).

how the reflection coefficients r_1, r_2 on the two sides of the film depend on the magneto-optical parameter Q (cf. Ref. 17). Here $\delta^E = a\epsilon'_{2r} + b\epsilon'_{2i}$ and $\delta^{ell} = b\epsilon'_{2r} - a\epsilon'_{2i}$ characterize the EKE and the ellipticity of a bulk sample,

$$\begin{aligned} a &= 2N^2 [A_1 / (A_1^2 + B_1^2)] \sin 2\varphi, & b &= 2N^2 [B_1 / (A_1^2 + B_1^2)] \sin 2\varphi, \\ A_1 &= \epsilon_{2i} (2\epsilon_{2r} \cos^2 \varphi - N^2), \\ B_1 &= (\epsilon_{2i}^2 - \epsilon_{2r}^2) \cos^2 \varphi + N^2 (\epsilon_{2r} - N^2 \sin^2 \varphi), \\ q &= [N^2 (N^2 \sin^2 \varphi - n^2) - n^4 \cos^2 \varphi] \\ & \quad [N^2 (N^2 \sin^2 \varphi - n^2) + n^4 \cos^2 \varphi]^{-1}, \\ n &= n + ik, & \epsilon_2' &= i\epsilon_2 Q, \end{aligned}$$

and $\epsilon_2 = \epsilon_{2r} + i\epsilon_{2i}$ and $\epsilon_2' = \epsilon'_{2r} + i\epsilon'_{2i}$ are the diagonal and off-diagonal components of the dielectric tensor of the surface-active medium, respectively. We used (6) and (8) to calculate the curves $R_p/R_s(\varphi)$ and $\delta_t^E(\varphi)$ for a thin nickel film with air- and water-filled cells. The dashed curves in Fig. 2 show these calculations for $\hbar\omega = 3.2 \text{ eV}$.

We note that the optical constants of thin ferromagnetic films are sensitive to the thickness (see, e.g., Ref. 18). For example, measurements of $n(t)$ and $k(t)$ for iron in Ref. 19 revealed that $n(t)$ increases with $1/t$, while k decreases. The curves $R_p/R_s(\varphi)$ and $\delta_t^E(\varphi)$ plotted in Fig. 2 were calculated for $n = 2.05$, $k = 2.56$, and $\epsilon_2' = 0.0325 + i0.101$, which differ somewhat from the values for the bulk material. The agreement between the calculated and experimental curves for air- and water-filled cells is seen to be quite good. Moreover, $\delta_t^E(\varphi)$ calculated in Ref. 17 for these same values of n, k , and ϵ_2' was also virtually identical to the experimental curve found for the same sample.

We will now discuss the measurements for Permalloy ($\text{Fe}_{20}\text{Ni}_{80}$) films of thickness 200 and 2000 \AA . Figures 3 and

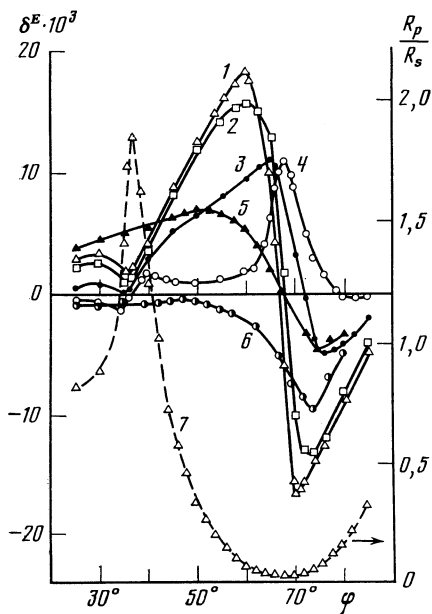


FIG. 3. Angular dependence $\delta^E(\varphi)$ for Permalloy ($\epsilon_3 = 1$). Curves 1–4 are for $t = 200 \text{ \AA}$, $\hbar\omega = 3.0, 2.5, 2.0$, and 1.5 eV ; 5, 6) $t = 2000 \text{ \AA}$, $\hbar\omega = 3.0$ and 1.5 eV ; 7) $R_p/R_s(\varphi)$, $t = 200 \text{ \AA}$, $\hbar\omega = 3.0 \text{ eV}$.

4 show $\delta^E(\varphi)$ for fixed $\hbar\omega$ for a 200-\AA -thick Permalloy film with air- and water-filled cells, respectively. Similar measurements were carried out for an oil-filled cell. The curves $\delta^E(\varphi)$ for the 2000-\AA -thick Permalloy sample are shown only in Fig. 3 (curves 5, 6), because in this case they were identical for all of the above configurations. The dashed curves in Figs. 3, 4 show typical dependences $R_p/R_s(\varphi)$ for a thin film. We see that total internal reflection at the second surface of the Permalloy film occurs at higher φ as the refractive index n_3 of the adjacent dielectric increases. The

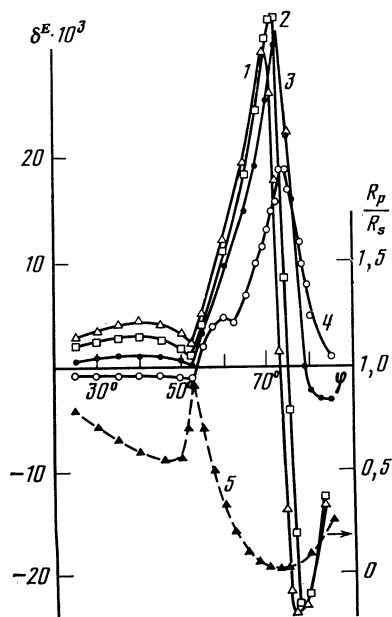


FIG. 4. Angular dependence $\delta^E(\varphi)$ for Permalloy ($\epsilon_3 = 1.77$), $t = 200 \text{ \AA}$. Curves 1–4 correspond to $\hbar\omega = 3.0, 2.5, 2.0$, and 1.5 eV , respectively; 5) $R_p/R_s(\varphi)$, $\hbar\omega = 3.0 \text{ eV}$.

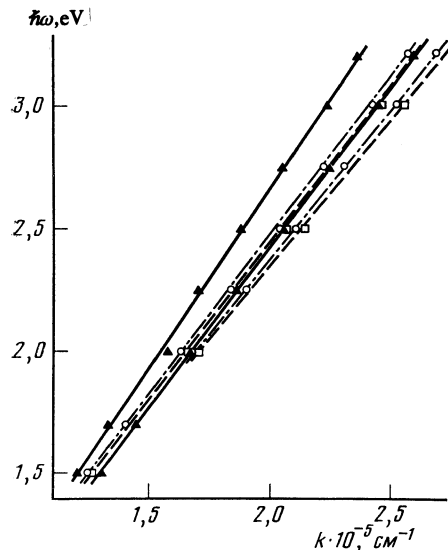


FIG. 5. Dispersion curves $k(\omega)$ for surface magnetoplasma waves in Permalloy; \blacktriangle , $\epsilon_3 = 1$; \circ , 1.77; \square , 2.29.

deep minimum on the curves $R_p/R_s(\varphi)$ may again be attributed to frustration of TIR by SPW excitation, while SMPW excitation is responsible for the abrupt increase in the magnetoreflexion δ .¹⁾

Figure 5 shows the SMPW dispersion $k(\omega)$ calculated by (2) from the data in Figs. 3, 4 and the corresponding measurements for an oil-filled cell. We see that $k(\omega)$ depends linearly on ω , and the two branches converge at $k = 0$ in the limit $\omega \rightarrow 0$. The splitting $\Delta(\hbar\omega)$ depends strongly on the optical properties of the dielectric at which the SPW and SMPW waves are excited. For air, $\Delta(\hbar\omega)$ varies from 0.15 to 0.3 eV for incident light energy $\hbar\omega = 1.5\text{--}3.2 \text{ eV}$, while for water and oil $\Delta(\hbar\omega)$ varies from 0.05 to 0.1 eV. Our experimental values $\Delta(\hbar\omega)$ for nickel and Permalloy films agree in order of magnitude with Ferguson's theoretical values,¹² which were calculated numerically with allowance for the dependence of the optical constants of the magnetic film on the thickness (this was done in order to bring the experimental and calculated curves $R_p(\varphi)$ into agreement). We will now attempt to explain qualitatively how ϵ_3 , the dielectric constant of the medium at whose boundary the surface magnetoplasma waves are excited, affects the splitting Δk for a transversely magnetized sample. The equations

$$\begin{aligned}
 M_1 M_4 - M_2 M_3 e^{-2\alpha_2 t} &= 0, \\
 M_1 &= k^2 \epsilon_1 / \alpha_1 + i \epsilon_2' k + \epsilon_2 (\alpha_2 - k_0^2 \epsilon_1 / \alpha_1), \\
 M_2 &= k^2 \epsilon_1 / \alpha_1 + i \epsilon_2' k - \epsilon_2 (\alpha_2 + k_0^2 \epsilon_1 / \alpha_1), \\
 M_3 &= -k^2 \epsilon_3 / \alpha_3 + i \epsilon_2' k - \epsilon_2 (\alpha_2 + k_0^2 \epsilon_3 / \alpha_3), \\
 M_4 &= -k^2 \epsilon_3 / \alpha_3 + i \epsilon_2' k - \epsilon_2 (\alpha_2 - k_0^2 \epsilon_3 / \alpha_3), \\
 \alpha_1^2 &= k^2 - k_0^2 \epsilon_1, \quad \alpha_2^2 = k^2 - k_0^2 \epsilon_2, \\
 \alpha_3^2 &= k^2 - k_0^2 \epsilon_3, \quad k_0 = \omega / c,
 \end{aligned} \tag{9}$$

were derived in Ref. 12 for the Kretschmann configuration ($K \parallel x \perp k$, film surface normal to the z axis); $\epsilon_2 = \epsilon_{2r} + i \epsilon_{2i}$, $\epsilon_2' = \epsilon_{2r}' + i \epsilon_{2i}'$, and k is the wave vector of the surface magnetoplasma wave. If we consider the saturation region of $k(\omega)$ (Ref. 9) and let $k \rightarrow \infty$, Eq. (9) simplifies to

$$\frac{(\varepsilon_1 + \varepsilon_2 + i\varepsilon_2')(\varepsilon_3 + \varepsilon_2 - i\varepsilon_2')}{(\varepsilon_1 - \varepsilon_2 + i\varepsilon_2')(\varepsilon_3 - \varepsilon_2 - i\varepsilon_2')} = 0. \quad (10)$$

Since the off-diagonal components of the dielectric tensor ε_2' of the film are at least an order of magnitude less than ε_1 , ε_2 , ε_3 , we get the relation

$$(\varepsilon_1 + \varepsilon_2)(\varepsilon_3 + \varepsilon_2) - i\varepsilon_2'(\varepsilon_1 - \varepsilon_3) = 0. \quad (11)$$

When combined with realistic approximations for $\varepsilon_2(\omega)$ and $\varepsilon_2'(\omega)$, Eq. (11) can be used to find the maximum frequency ω_s at which surface plasma waves can be excited; one can also calculate the change $\Delta\omega_s$ in ω_s , and hence also in the splitting Δk , produced when a magnetic field $\pm H$ is applied to the sample. Clearly, $\Delta\omega_s$ is determined by the last term in Eq. (11). We see that in qualitative agreement with the above results, $\Delta\omega_s$ decreases if we increase ε_3 .

We have thus studied the magneto-optical spectra of longitudinally and transversely magnetized nickel and Permalloy films with frustrated total internal reflection. The minima on the reflection curves are due to the excitation of surface plasma waves, while the extrema on the magnetoreflexion curves are associated with SMPW excitation. We have found that $k(\omega)$ splits into two branches for transversely magnetized samples ($H \perp k$), $k(\omega)$; for a specified energy $\hbar\omega$, the SMPW wave vector k on either of the branches can be reached by changing the angle of incidence of the light. In agreement with theoretical predictions, only one SMPW branch is observed for longitudinally magnetized samples. The SMPW dispersion equations were calculated for incident light energies 1.5–32 eV. An increase in ε_3 , the dielectric constant of the material at whose boundary the SPW and SMPWs are excited, is accompanied by an increase in the SMPW wave vector k and by a decrease in splitting Δk produced by an applied magnetic field $\pm H$.

In closing, we thank V. I. Zhilin for help in fabricating the samples.

¹⁾Curves 4 in Figs. 3,4 have additional weak peaks at $\varphi = 40$ and 60° , which may be attributed to excitation of an additional SMPW branch. Such branches could correspond to virtual polaritons, which were predicted theoretically in Ref. 1 (p. 111) and observed experimentally in Ref. 10.

¹⁾Polaritons, Proc. First Taormina Res. Conf. Struc. Matter (E. Burstein and F. de Martini, eds.), Pergamon Press, New York (1974).

²⁾Surface Polaritons, Electromagnetic Waves at Surfaces and Interfaces (V. M. Agranovich and D. L. Mills, eds.), North-Holland (1982).

³⁾V. M. Agranovich, Usp. Fiz. Nauk **115**, 199 (1975) [Sov. Phys. Usp. (1975)].

⁴⁾H. Raether, Phys. Thin Films **9**, 145 (1977).

⁵⁾A. Otto, Z. Phys. **216**, 398 (1968).

⁶⁾E. Kretschmann, Z. Phys. **241**, 313 (1971).

⁷⁾D. L. Mills and A. A. Maradudin, Phys. Rev. Lett. **31**, 372 (1973).

⁸⁾J. W. Chiu and J. J. Quinn, Nuovo Cim. **10B**, 1 (1972).

⁹⁾H. Kaplan, E. D. Palik, R. Kaplan, and R. Gammon, J. Opt. Soc. Am. **64**, 1551 (1974).

¹⁰⁾A. Harstein and E. Burstein, Sol. St. Comm. **14**, 1223 (1974).

¹¹⁾V. S. Ambrazyavichene and R. S. Brazis, Fiz. Tekh. Poluprovodn. **12**, 1114 (1978) [Sov. Phys. Semicond. **12**, 661 (1978)].

¹²⁾P. E. Ferguson, O. M. Stifford, and R. F. Wallis, Physica **86-88B**, 1403 (1977).

¹³⁾P. E. Ferguson, O. M. Stifford, and R. F. Wallis, Physica **89B**, 91 (1977).

¹⁴⁾G. S. Krinchik, E. E. Chepurova, and Sh. V. Égamov, Zh. Eksp. Teor. Fiz. **74**, 714 (1978) [Sov. Phys. JETP **47**, 375 (1978)].

¹⁵⁾N. J. Harrick, *Internal Reflection Spectroscopy*, Interscience, New York (1967).

¹⁶⁾G. S. Krinchik, E. E. Chepurova, and T. I. Kraeva, Pis'ma Zh. Eksp. Teor. Fiz. **40**, 47 (1984) [JETP Lett. **40**, 776 (1984)].

¹⁷⁾A. V. Druzhinin, I. D. Lobov, V. M. Maevskii, and G. A. Bolotin, Fiz. Met. Metalloved. **56**, 58 (1983).

¹⁸⁾H. Judy, IEEE Trans. Magn. **MAG-6**, 563 (1970).

¹⁹⁾H. Stremme, Diploma Thesis, Phys. Dept., Univ. Munich, Germany (1969).

Translated by A. Mason